INTERACTION BETWEEN TUNDISH GUNNING MATERIALS AND LIQUID STEEL

Yu Liu[1], Guangqiang Li[1, 2], Li Wang[2], Zhao Zhang[2], Zhizheng Yang[2,3], Jiangping Rao[2,3]
1 The State Key Lab. of Refractories and Metallurgy, Wuhan University of Science and Technology, China
2 Key Lab. for Ferrous Metallurgy and Resources Utilization of Ministry of Education, Wuhan University of Sci. and Tech., China
3 Wuhan Iron and Steel Company Limited, China Baowu Steel Group Limited, China
liguangqiang@wust.edu.cn

ABSTRACT

To clarify the interaction mechanism between distinct tundish gunning materials (GM) and liquid steel, two kinds of gunning materials, namely MgO, Al_2O_3 based GM were tested. SEM, EDS, XRD and chemical analysis were carried out for steel and GM to investigate the change of chemical composition of steel in contact with GM and the interface microstructure between steel and GM after high temperature holding experiments. The steel cleanliness in terms of inclusion number density and size distribution was evaluated. The results show that the reducible component, low-melting-point phases and the pores in GM are passageway for steel penetration. The Al_2O_3 GM is less prone to steel penetration due to its poor wetting and the dense transition layer. MgO GM shows a stronger oxidizing capacity due to its higher content of reducible impurity oxides (10.5 wt.% SiO_2+2 wt.% Fe_2O_3). The use of Al_2O_3 GM results in an improved steel cleanliness and consequently could be a promising refractory in the tundish lining.

Keywords: tundish; gunning materials; interaction; steel; cleanliness

INTRODUCTION

In order to reduce the wear of tundish refractory and the reoxidation of molten steel, gunning materials (GM) are commonly used in the inner surface layer of tundish as a dispensable protective layer between the main tundish refractory and the molten steel inside tundish. Although gunning materials is in contact with steel for 16 to 24 hours, it affects the steel cleanliness due to its direct contact with molten steel after the refining. Currently, the MgO GM is widely used and studied. The Al_2O_3 GM is relative less used and studied. Pengcheng Yan *et al.* investigated the interaction between Al_2O_3 GM and an Ti killed ultra low carbon steel [1]. They found the Al_2O_3 GM was less prone to steel infiltration than MgO GM. However, the phase of Al_2O_3 GM after interaction has been not studied. In the present work, two types of gunning materials, namely MgO, Al_2O_3 GM were tested. The interactions between gunning materials and liquid steel, including chemical reactions, steel penetration, refractory corrosion, the phases and the oxidizing capacity of gunning materials were investigated. The effect of gunning materials on the composition and inclusions (composition, number density and size distribution) of steel was studied as well.

EXPERIMENT

Table 1 and 2 show the chemical compositions of the steel and gunning materials, respectively. Al-killed ultra low carbon and nitrogen steel was placed in an alumina crucible (OD＝50 mm) coated with a layer of gunning materials. Thickness of gunning materials layer is about 7 mm, the contact area between GM and 200 g molten steel is about 25.92 cm^2, the density of MgO and Al_2O_3 GM at room temperature is about 3433 and 3496 kg/m^3, respectively. The crucible was placed in a graphite crucible (ID=55 mm) and heated to 1550 ^oC in a vertical tube furnace (heating elements: $LaCrO_3$ bars) for 2 hours under Ar atmosphere (flow rate: 3.4×10^{-6} m^3/s). Four steel samples were taken by sucking with quartz tube (ID=4 mm) from the position closing to the bottom center of molten steel in crucible at 30 min, 60 min, 90 min and 120 min for inclusion and composition analysis. After 2 hours of holding, the furnace was cooled to room temperature and then crucible was then taken out of the furnace.

Tab. 1: Chemical composition of steel used (mass %)

C	Si	Mn	P	S	Al_s	Ti	Mg	N
0.003	0.013	0.077	0.012	0.008	0.039	0.067	0.004	0.002

Tab. 2: Chemical composition of gunning materials (mass %)

No.	Type	MgO	CaO	SiO_2	Al_2O_3	Fe_2O_3
I	MgO	78	6.1	10.5	3.6	2
II	Al_2O_3	-	1.3	3.3	93.4	2

Sample involving steel/GM interface was embedded in an epoxy resin and polished. The microstructure and composition of the specimens were analyzed by a FE-SEM with EDS. The phase change of the refractory was analyzed by means of X-ray diffractometer. The composition of the steel samples were measured by ICP-AES and Oxygen and Nitrogen Analyzer, the inclusions assessment was carried out by a Image Pro-Plus 6.0 software with photos from 30 randomly visual fields of the SEM at 2000 magnification.

RESULTS AND DISCUSSION

Composition Change of Molten Steel

The compositional change of the steel as a function of time is shown in Fig. 1, which depicts a clear overview of oxidation sequence for each element in molten steel, that is firstly [Al], followed by the [Ti], [Si], and [Mn]. In both tests, the [Al] content rapidly drops within 30 minutes, and then stays constant at this level until the test finishes. A large amount of [Si] pick-up is observed simultaneously with the rapid decrease in [Al] and [Ti] contents in the beginning of the test, implying that SiO_2 in the GM is reduced by Al and Ti in molten steel as Eqs. 1 and 2. Afterward the [Al] and [Ti] are depleted, the [Si] and [Mn] start to combine with oxygen as Eq. 3. The [Ti] content drops slower in test of Al_2O_3 GM. The [Mn] content decreases slightly in both tests. The Mg content increases in the test of MgO GM, whereas, keeps a constant in the test of Al_2O_3 GM. The T.O (Total oxygen including oxygen dissolved in iron and as oxide inclusions) content in steel analyzed by Oxygen and Nitrogen Analyzer at 30 min is around 95 ppm using MgO GM, rapidly drops to around 60 ppm and then follows a slow increase until the test finishes. The T.O content in steel at 30 min is around 120 ppm using Al_2O_3 GM, rapidly drops to around 55 ppm and then follows a slow decrease. After 30 min, the T.O content of steel is lower in test with Al_2O_3 GM. A nitrogen pick-up is observed and similar in both experiments. After 2 h holding, the lower [Al], [Ti], [Mn], [Si] final contents and higher T.O contents of steel in the test with MgO GM implies that MgO GM has a stronger oxidizing capacity due to its higher reducible components (10.5 wt.% SiO_2 + 2 wt.% Fe_2O_3).

$$4[Al] + 3SiO_2 \rightarrow 3[Si] + 2Al_2O_3 \quad (1)$$

$$[Ti] + SiO_2 \rightarrow [Si] + TiO_x \quad (2)$$

$$[Al, Ti, Si, Mn] + Fe_2O_3 \rightarrow Fe + (Al, Ti, Si, Mn)O_y \quad (3)$$

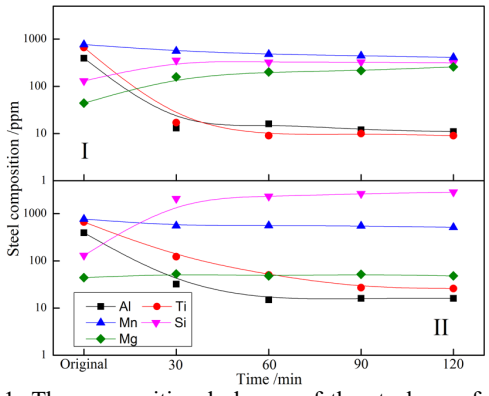

Fig. 1: The compositional change of the steel as a function of holding time for different gunning materials: I-MgO based gunning materials; II-Al_2O_3 based gunning materials.

The Number and Size Distribution of Inclusion in Steel

Table 3 shows the results of inclusion statistics in steel samples. It should be noted that inclusions less than 0.5 μm were not counted due to the accuracy of the Image Pro-Plus 6.0 software. It can be seen from Table 3 that the inclusion number in the test of Al_2O_3 GM is less than that in the case of MgO GM. In order to analyze the distribution of inclusions in detail, the volume fraction of inclusions is calculated according to Ref. [2]. As shown in Table 3, the volume fraction of inclusions decreases from 30 min to 120 min in the test of MgO GM. In case of Al_2O_3 GM, the volume fraction of inclusions also decreases during whole experiment. Compared to the test of MgO GM, the volume fraction of inclusions is lower in the test of Al_2O_3 GM, implying a better steel cleanliness. The average size of inclusions is larger in the case of Al_2O_3 GM because magnesia in liquid steel grows slowly [3] and the alumina is prone to aggregate and grow up.

Tab. 3: Inclusion statistics in steel samples at different time

No.	Time (min)	N (mm^{-2})	V (10^{-4} %)	D (μm)	Size distribution/%		
					< 1μm	1～3μm	> 3μm
I-1	30	626	1.90	1.19	49.2	49.2	1.6
I-2	60	777	1.59	0.91	77.2	22.1	0.7
I-3	90	469	0.97	0.96	71.7	27.7	0.6
I-4	120	407	0.80	0.92	76.9	21.2	1.9
II-1	30	388	1.25	1.20	46.3	50.3	3.4
II-2	60	461	0.95	0.94	71.8	27.1	1.1
II-3	90	263	0.55	1.00	71.4	26.7	1.9
II-4	120	239	0.54	0.96	72.0	27.3	0.7

Note: I-MgO GM, II-Al_2O_3 GM, N- number density of inclusions, V-volume fraction of inclusions, D-average diameter of inclusions.

The SEM and EDS images of inclusion in steel closed to the steel/GM interface are shown in Fig. 2. The large inclusions closed to the steel/refractory interface with irregular shape have a similar composition and structure as the gunning materials, indicating they are the results of gunning materials erosion.

Microstructure Characterization of the Steel/GM Interface and the Phase Change of the GM

After 2 h contacting with liquid steel, the remained thickness of MgO GM is thinner than that of Al_2O_3 GM. Figs. 3a and c show the microstructure of the steel/refractory interface. Lots of fine iron particles (the white dot in Figs. 3a and c) exist in GM near the steel/GM interface because the molten steel infiltrates into the gunning materials. The infiltration layer thickness of Al_2O_3 GM is about 200 μm, however, that of MgO GM is about 1.2 mm. The SEM image of corroded gunning materials is shown in Figs. 3b and d. It can be observed that MgO GM has two layers, infiltrated and origin one, Al_2O_3 GM has three layers, infiltrated, transition, and origin one. The SEM image and EDS elements mapping of corroded MgO and Al_2O_3 GM are shown in Fig. 4. It should be noted: in order to ensure the original morphology of the Al_2O_3 GM and avoid abrasive materials (Al_2O_3 powder) into the pore, the Al_2O_3 GM was not grinded and polished. Figs. 4a-d indicates that the steel infiltration damages the integrity of MgO GM. The same phenomenon is found in the Al_2O_3 GM (Figs. 4e-h). The iron particles mainly exist in the surface of the Al_2O_3 GM, whereas, the severer and deeper steel infiltration occurs in the MgO GM, resulting in larger iron particles and severer structure damage in the MgO GM. The differences of Mg mapping over the observed region are caused by the steel infiltration and the cracks (formed by thermal shock during cooling or mechanical load during sample preparation) in GM.

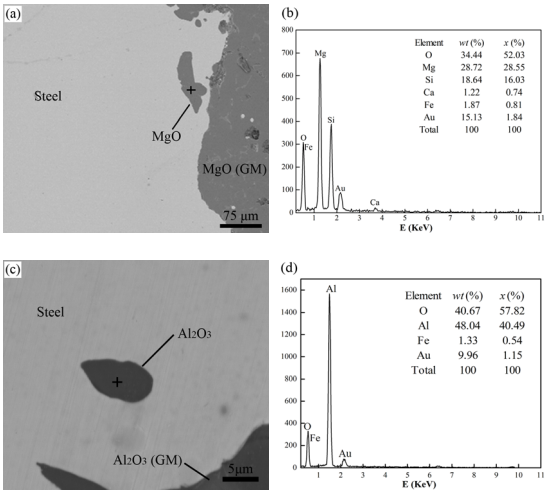

Fig. 2: The SEM (a,c) and EDS (b,d) images of inclusion in steel closed to the steel/GM interface after the test: MgO GM (a, b), Al_2O_3 GM (c, d).

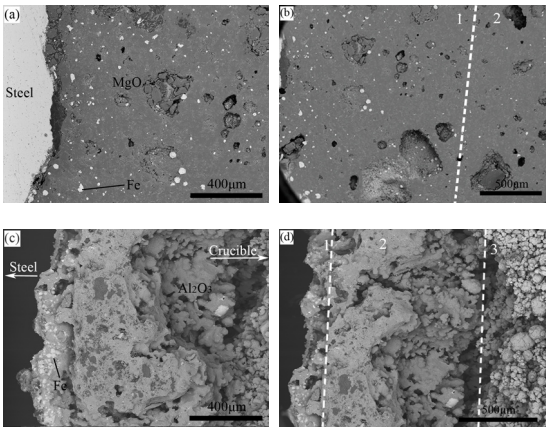

Fig. 3: SEM images of the steel/GM interface (a,c) and corroded gunning materials (b,d)：a,b-MgO based gunning materials with severe infiltration (b-1 infiltrated layer, b-2 original layer); c,d-Al_2O_3 based gunning materials with moderate infiltration (d-1 infiltrated layer, d-2 transition layer, d-3 original layer).

XRD patterns of GM after experiment are presented in Fig. 5. The hot face is closed to molten steel. The phase composition of hot face and the original layer after test are nearly the same in the MgO GM (Fig. 6a). Compared with the original layer, single SiO_2 phase is not found in the hot face of Al_2O_3 GM, this is because the SiO_2 exists in other phases as shown in Fig. 5b. The calculated melting points of Fe_2SiO_4, $CaMgSi_2O_6$, $CaFe_2O_4$ and $CaFeSi_2O_6$ are 1211.1 °C, 1376.6 °C, 1229.7 °C and 1173.1 °C

by using the Equilibrium module of the FactSage 6.1 with the database of FToxid, respectively. The low-melting-point phase is existed in both MgO and Al_2O_3 GM.

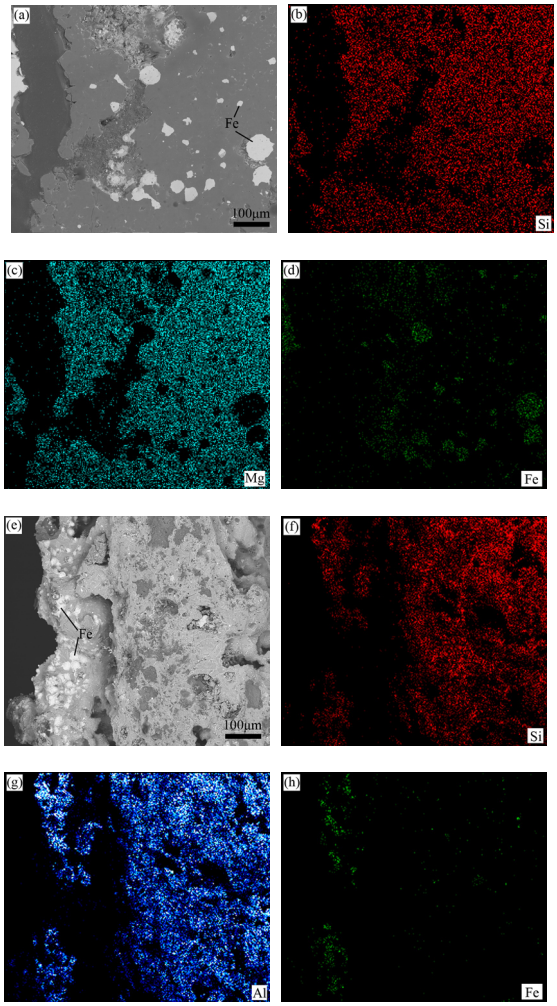

Fig. 4: SEM and EDS elements mapping images of corroded MgO (a-d) and Al_2O_3 (e-h) based gunning materials, (b, f): Si; (c): Mg; (g): Al; (d, h): Fe.

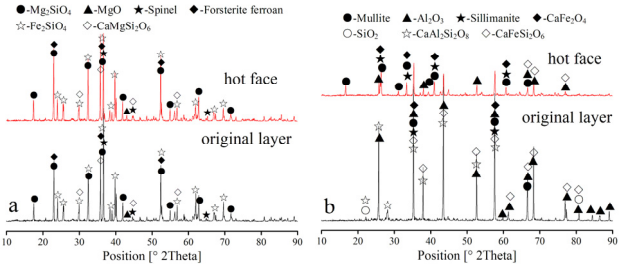

Fig. 5: XRD patterns of the hot face and the original layer after experiment: a-MgO based gunning materials; b-Al_2O_3 based gunning materials.

According to the above experimental results, the corrosion mechanism of GM can be explained as follows: (a) Molten steel contacts with GM, but doesn't start to react. (b) SiO_2 and Fe_2O_3 in the surface of GM are reduced by the dissolved Al, Ti, Mn and Si in molten steel, leading to formation of the inclusions in steel; oxides with lower melting point may flow into molten steel, spaces remained will be infiltrated by molten steel. Moreover, the pores and low-melting-point phase oxides become the passageway for steel infiltration. (c) Further steel infiltration damages the integrity of GM at high temperature. (d) Particles of GM falls into molten steel to form the large inclusion due to the structure damage of the GM, these large inclusions have a similar composition as the GM as confirmed by Fig. 2.

The low melting point phase and molten steel flow into the interparticle pores and subsequently penetrate into the compact particle boundaries [4]. Finally, the high melting point particles (Al_2O_3) are surrounded by the liquid phase and dissolved into the molten oxide mixture at high temperature, resulting in a higher viscosity and worse fluidity in the molten oxide mixture. With more particles dissolved into the oxide mixture, the liquid phase becomes more viscous to blocking the pores [5]. This is the formation mechanism of the dense transition layer, which slows down the material transfer in gunning materials and prevents further steel infiltration. Compared with MgO GM, the contact angle between molten steel and Al_2O_3 GM is larger ($\theta > 140^o$) [6, 7]. Therefore, the Al_2O_3 GM is found to be less prone to steel penetration due to its poor wetting and the dense transition layer. The lager iron particles and severer structure damage occurs in the MgO GM. The refractory materials particle drops into liquid steel, resulting in an increase in Mg content in test of MgO. The residual thickness of MgO GM is thinner after 2 h experiments.

CONCLUSIONS

SiO_2 and Fe_2O_3 in gunning materials are reduced by the dissolved Al, Ti, Mn and Si in molten steel, and then liquid steel penetrates into the sites where they locate, resulting in steel infiltration. The pores and low melting point phases in gunning materials also provide the passageway for steel infiltration. The steel infiltration damages the integrity of gunning materials, as a result, the refractory materials particles fall into liquid steel to become large-sized inclusions. The Al_2O_3 GM is found to be less prone to steel penetration due to its poor wetting with molten steel and the dense transition layer. The MgO GM with higher reducible content (10.5 wt.% SiO_2+2 wt.% Fe_2O_3) has a stronger oxidation capacity than Al_2O_3 GM. Al_2O_3 GM could be a promising GM in the tundish due to less contamination into the molten steel.

REFERENCES

[1] Yan P, Van MA, Zinngrebe S, Laan S, Blanpain B, Guo M. Interaction between steel and Distinct Gunning materials in the tundish. ISIJ Int. 2014; 54: 2551-8.

[2] Goto H, Miyazawa K, Tanaka K. Effect of oxygen content on size distribution of oxides in steel. ISIJ Int. 1995; 35: 286-91.

[3] Ohta H, Suito H. Dispersion behavior of MgO, ZrO_2, Al_2O_3, CaO-Al_2O_3 and MnO-SiO_2 deoxidation particles during solidification of Fe-10 mass % Ni Alloy. ISIJ Int. 2006; 46: 22-8.

[4] Wei Y, Li N, Ke C. Effect of silicon carbide on reactions between molten steel and fused magnesia-silicon carbide composite refractory. Am Ceram Soc Bull. 2007; 86: 9201-5.

[5] Scheunis L, Mehrjardi AF, Campforts M, Jones PT, Blanpain B, Jak E. The effect of phase formation during use on the chemical corrosion of magnesia-chromite refractories in contact with a non-ferrous PbO-SiO_2 based slag. J Eur Ceram Soc 2014; 34: 1599-610.

[6] Huang XH. Principles of Ferrous Metallurgy. 3rd ed. Beijing: Metallurgical Industry Press; 2012. (in Chinese)

[7] Poirier D, Yin H, Suzuki M, Emi T. Interfacial properties of dilute Fe-OS melts on alumina substrates. ISIJ Int. 1998; 38: 229-38.